Composites Part B 117 (2017) 138–149

Contents lists available at ScienceDirect

Composites Part B

journal homepage: www.elsevier.com/locate/compositesb

Dimensional accuracy analysis of coupled fused deposition modeling and vapour smoothing operations for biomedical applications

Jasgurpreet Singh Chohan [a], Rupinder Singh [b], Kamaljit Singh Boparai [c], Rosa Penna [d], Fernando Fraternali [d, *]

[a] I.K.G. Punjab Technical University, Kapurthala, 144601, India
[b] Production Engineering Department, GNDEC, Ludhiana, 141006, India
[c] Mechanical Engineering Department, MRSPTU, Bathinda, 151001, India
[d] Department of Civil Engineering, University of Salerno, Italy, 84084, Fisciano, SA, Italy

ARTICLE INFO

Article history:
Received 14 January 2017
Accepted 28 February 2017
Available online 6 March 2017

Keywords:
Vapour smoothing
Dimensional accuracy
Fused deposition modeling
ABS replicas
Hip prostheses

ABSTRACT

Fused Deposition Modeling (FDM) is one of the most extensively used Additive Manufacturing technique which has substantially shortened the product development time and cost. The application has been extended to fabricate biomedical implants through investment casting process. But the FDM replicas exhibit poor surface quality which requires further post finishing. Thus, it is very difficult to achieve adequate dimensional accuracy as surface finishing techniques resulted in material removal and erosion of upper surface. The vapour smoothing is an advanced finishing technique which eliminates tool-workpiece contact and yield ultra smooth finish but dimensional accuracy of FDM replicas is yet to be ascertained. In present research, the efforts are made to explore the influence of FDM and VS process parameters in dimensional features of complex designs. The influence of six parameters on radial (head diameter) and linear dimensions (neck and stem thickness) is studied using Taguchi orthogonal array. The CMM measurements showed shrinkage in head diameter while positive deviation has been observed in linear dimensions before vapour smoothing with maximum impact of orientation angle. The vapour smoothing process caused shrinkage in both linear and radial dimensions with maximum effect of smoothing time. The process parameters and their levels are optimized and confirmatory experiments indicated reduced deviations in dimensional features with consistency in IT grades.

1. Introduction

Additive Manufacturing (AM) is the set of advanced manufacturing techniques which works through layer by layer joining of materials opposed to subtractive techniques used in traditional manufacturing processes [1]. The AM techniques are extending their applicability from functional and aesthetic prototypes to production of tools for direct use. The new field of Rapid Tooling has been emerged which satisfies the competitive market demands of low cost products with shorter lead times [2]. Moreover, precise and intricate shapes can easily be manufactured through AM which can be further used as sacrificial patterns (replicas) for investment casting (IC). The plastic patterns, cores and risers required for IC can be manufactured directly through AM technique within few hours. The investment casting process ensures efficient and economical route to produce components with high precision and surface finish [3]. The applications of AM have been intensively applied to production of dental implants, artificial limbs, surgical implants, jewellery and turbine blades. The process has potential to revolutionise the biomedical research with production of patient specific customized implants. The three dimensional images of damaged bones can be fed as input and plastic replicas are prepared through additive manufacturing for further casting [4].

Fused Deposition Modeling (FDM) developed by Stratasys. Inc. has been specifically nominated by researchers due to its flexibility and simplicity as compared to other AM techniques [5]. The scanned data or 3D drawing of object in STL format is fed as input to FDM. In FDM technology, the plastic material is extruded in semi-molten form by a nozzle moving in X and Y direction on

* Corresponding author.
E-mail addresses: jaskhera@gmail.com (J.S. Chohan), rupindersingh78@yahoo.com (R. Singh), kamaljitboparai2006@yahoo.co.in (K.S. Boparai), rpenna@unisa.it (R. Penna), f.fraternali@unisa.it (F. Fraternali).

http://dx.doi.org/10.1016/j.compositesb.2017.02.045
1359-8368/

fixtureless table (Fig. 1). As one layer is deposited, the nozzle head is numerically raised (in Z direction) to deposit subsequent layers. The other nozzle extrudes support material which acts as scaffolding and can be easily removed afterwards [6].

Unfortunately, one of the biggest limitations of this process is poor surface finish which arises due to chordal error and stair-stepping [7]. Various pre-processing (before fabrication) techniques have been applied to achieve minimum surface roughness such as adaptive slicing and optimization of process parameters [8]. These techniques cannot improve the surface finish beyond certain limit as roughness is an inherent defect. Furthermore, the chordal error and staircase effect also impart considerable dimensional variability in FDM parts [9]. The poor surface finish and dimensional accuracy of replicas is inherited by casting when used in investment casting process. The slight variation in dimensions of implants can lead to post-operative complications in patients [10]. Thus, it is obligatory to improve the surface finish and dimensional accuracy of finished replicas before recommending the procedure for bio-medical application.

The Post-Processing (after fabrication) techniques have been adopted by various researchers such as manual polishing, barrel finishing, abrasive flow machining and vibratory finishing. These mechanical finishing materials are quite effective but induce dimensional variability in parts. Moreover, intricate details, thin sections and corners are damaged due to mechanical forces acting on plastic parts [11].

The chemical finishing method was experimented [12] where FDM parts are immersed in acetone solution (90% acetone and 10% water) for 5 min. The measurements shower excellent surface finish with 1% reduction in dimensions and 1% increase in average weight. Recently, the researchers [13] used fan to circulate the acetone vapours over FDM parts for surface finishing. The surface roughness is reduced with an increase in rotations of fan while longer exposure is required to finish ABS parts with larger surface area. Garg et al. [14] utilized of cold acetone vapours (at 20 °C) to finish ABD parts made by FDM. The part surface quality is improved when exposure duration is increased is with minute dimensional changes. During longer exposure (90 min), the sharp edges and corners are rounded off due to erosion by chemical vapours. The uncontrolled use of volatile chemicals could potentially damage the fine details of plastic parts as chemical fumes abruptly attack the corners and thin sections.

The surface finish and dimensional accuracy of FDM parts are inter-related as parts with high surface roughness promoted dimensional errors. The attempts made to improve the surface quality further deteriorate the dimensional accuracy of ABS parts. Thus, there is need to develop a systematic procedure which can simultaneously improve both surface finish and dimensional accuracy of FDM parts.

An advanced finishing process known as vapour Smoothing (VS) has been developed by Stratasys, Inc. where the hot chemical vapours react with upper surface of FDM parts. The preliminary research has been performed on standard geometries (test parts) regarding dimensional accuracy by Espalin et al. [15]. The study reported minimal dimensional variations in test parts after vapour exposure. The system provides the controlled environment for vaporization of specialized chemical (compatible for ABS) which ensures negligible damage to part surface.

However, to thoroughly validate the FDM-IC route for production of biomedical implants, it is mandatory to investigate the dimensional behaviour of actual part geometries under this VS system. The present study would explore the effects of vapour smoothing on dimensional accuracy of replicas of biomedical implants. Moreover, the study would focus to optimize various process parameters of combined FDM-VS processes to achieve consistent and minimum dimensional variation as required for mass production.

2. Methodology

2.1. Materials and equipments

For present study, the replica of hip implant (Fig. 2) has been selected as benchmark which is designed in “Solidworks 2014”. The hip joint is a ball and socket joint which connects pelvis and thighbone. The sloping profile and intricate geometrical features of hip implant led to test the efficacy of vapour smoothing process. The three target locations are selected based on constructional features, significance, shape and size. The diameter of head (ball of

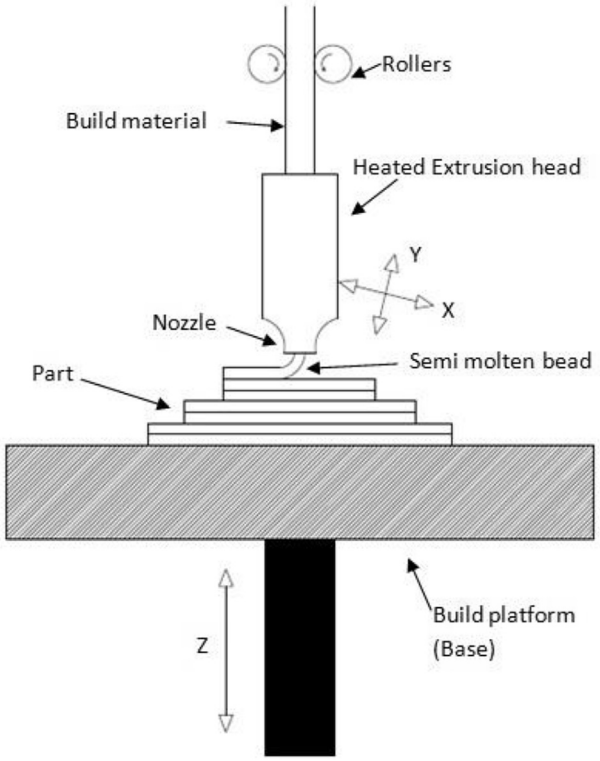

Fig. 1. Schematic diagram of Fused Deposition Modeling apparatus.

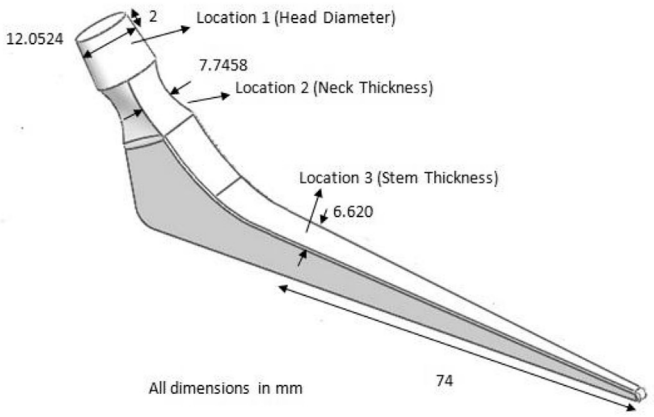

Fig. 2. Benchmark component of hip joint.

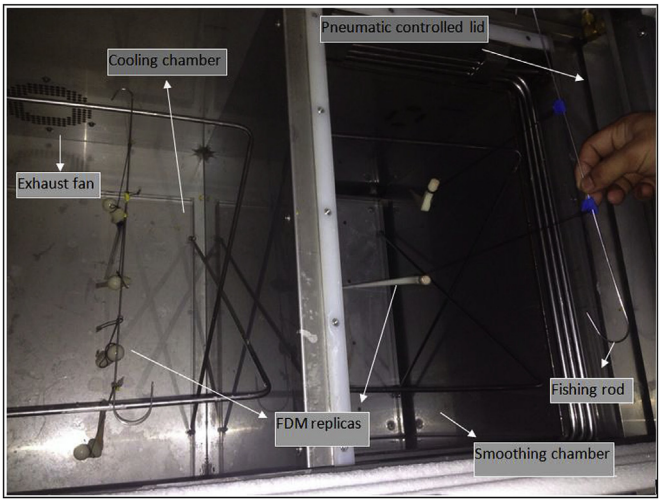

Fig. 3. Schematic of vapour smoothing process.

hip joint) is marked as location 1. Since the diameter varies with distance, the target location is highlighted at 2 mm distance from top. The location 2 is in the middle section of neck whose thickness is measured whereas location 3 is stem thickness.

The stem thickness is measured at distance of 74 mm from end of stem. The original dimensions at these locations are retrieved from CAD data using Solidworks 2014. The actual measurements of these three features are taken before and after chemical vapour smoothing which are compared with original (CAD) dimensions afterwards. The Coordinate Measuring Machine Crysta-Apex C163012 supplied by Mitutoyo with 0.1 μm resolution has been configured testing the dimensional measurements as per ISO 10360–2:2009 regulations [16]. The length, diameter and thickness and elevation of various features have been surveyed by 113 touch points.

To correlate the efficacy of finishing process, the surface roughness profiles have been acquired in addition to dimensional accuracy measurements. The surface profiles are plotted with "Mitutoyo-SJ-210" roughness tester using employing Gaussian filter at cut-off length 0.25 mm and exploratory length 2.5 mm as per ISO 4287 regulations [17].

The conversion of 3d file in STL format, slicing and toolpath generation has been done by "CatalystEx". The ABS-P400 plastic material has been utilized to manufacture replicas in "uPrint SE" commercial FDM apparatus (make: Stratasys Inc., USA).

The chemical vapour finishing has been performed with "Finishing Touch Smoothing Station" supplied by Stratasys Inc., USA having two chambers i.e. cooling chamber and smoothing chamber as shown in Fig. 3. The parts are hanged alternately in these two chambers for specific durations for finishing (specifications in Table 1).

The smoothing chamber has heaters beneath maintained at 65 °C where smoothing fluid is constantly heated to vaporize and react with upper surface of parts [18]. The smoothing chamber is covered by a pneumatic controlled lid operated by foot switch to avoid the exhaust of vapours outside. The cooling coils run around top surface of smoothing chamber which condense and re-circulate the evolving vapours. The smoothing fluid (specifications in Table 2) is highly volatile liquid as the fumes can be smelled even at room temperature [19]. Initially, the parts are pre-cooled (hanged) in cooling chamber which is maintained at 0°c followed by exposure in smoothing chamber. At last, the parts are again hanged in cooling chamber for post-cooling. The exhaust fan has been installed at bottom of the cooling chamber which pushes the extra vapour fumes outside.

2.2. Selection of input parameters

As revealed by literature, the dimensional accuracy of parts significantly depends upon FDM pre processing parameters [8,11]. Moreover it required to study the combined effect of FDM and VS processes on dimensional variability of finished parts. Thus, for present study two pre-processing parameters have been selected as input i.e. orientation angle and part density. The orientation angle is most important parameter which effects surface finish, build time, mechanical strength and dimensional accuracy of parts [7]. Thus, two levels of orientation angles i.e. 0° and 90° are selected which have potential to yield maximum surface finish, accuracy and strength [9]. The previous researchers reported [13,14] detrimental effects of chemical vapours on upper surface of ABS parts which may differ with material density. The FDM apparatus has capacity to fabricate parts with three different densities i.e. normal, sparse and dense based on different interior fill styles. So, the part density was selected as second pre-processing input parameter with three levels.

The range of post-processing parameters (for vapour smoothing apparatus) has been worked out on basis of operation manual [18] and pilot experiments. The manufacturer recommends pre-cooling the parts for 10–20 min and then smoothing for 10–30 s. Afterwards, the post-cooling for 10–20 min is recommended. Moreover it is recommended to repeat the whole cycle i.e. precooling-smoothing-postcooling twice or thrice till required finish is achieved. The vapour pressure, concentration of smoothing fluid, temperature of smoothing and cooling chamber could not be changed as recommended by manufacturer. Thus, only pre-cooling, post-cooling and smoothing times and their repetition (cycles) can be varied in present investigation. The pilot experiments revealed swelling and blow-holes on surface of ABS replicas when exposed beyond 25 s in smoothing chamber. The final range of selected parameters for experimentation has been shown in Table 3.

Table 1
Specifications of vapour smoothing apparatus.

Manufacturer	Stratasys Inc., USA
Model	Finishing Touch Smoothing Station
Vapour smoothing system size (LxBxH)	1333.5 × 812.8 × 1168.4 mm
Vapour smoothing system weight	182 kg
Smoothing/cooling chamber size (LxBxH)	330 × 406 × 508 mm
Power requirements	200-240 V AC, 50/60 Hz, 20 amp
Smoothing chamber temperature range	45-50 °C
Smoothing chamber heater temperature	65 °C
Cooling chamber temperature range	0-4 °C
Cooling coils (Refrigeration) temperature	0 °C
Operating Range	Ambient temperature 15.6 °C –29.4 °C

Table 2
Specifications of smoothing fluid.

Manufacturer	Microcare Corporation, USA
Product No.	MCC-SSF01P
Boiling point	43 °C
Storage temperature (Max.)	52 °C
Ingredients and Composition	1,1,1,2,3,4,4,5,5,5-Decafluoropentane (10–30%) *Trans*-Dichloroethylene (60–100%)
Colour/Odour	Clear & Colourless/Slight odour
Volatility Description	Volatile (100% by vol.)
Solubility	Slightly soluble in water
Flammability	Non flammable (Min. 7% and Max. 14%)
Vapour density	<1
Weight/ml at 20 °C	0.984 gm

The successive cooling and heating (smoothing) of parts may produce errors in the estimations due to interaction. Thus, the interaction effects between input parameters are also studied.

The environmental factors like ambient temperature, humidity and air circulation are considered noise factors which are difficult to control during experimentation. The noise factors can bring undesired variation (noise) in results which must be eliminated using robust design of experiments technique.

2.3. Experimental design matrix

The cautious planning and execution of experiments is of utmost importance to derive the accurate and clear conclusions from observed data. The present research focused on creating robust experimental design for surface finishing process of ABS replicas of biomedical implants aiming for minimum dimensional variability. Furthermore, the study aspires to establish the relationship between various pre-processing and post processing parameters with dimensional accuracy of replicas.

The Taguchi technique has been utilized to design experiments to evaluate the performance of vapour smoothing process and minimizing impact of noise factors so as to achieve consistent dimensional accuracy. The Taguchi Orthogonal arrays (OA) are most frequently used technique involving smaller number of experiments but yielding good results. In present study, total six input parameters are chosen out of which one has two levels while other five have three levels each. The minimum number of experimental runs required for Taguchi OA have been calculated using the formula given below [20]:

$$\text{Number of experiments} = [(L-1)*P] + 1 \quad (1)$$

where L is number of levels and P is number of parameters.

Considering six parameters with three levels (maximum), minimum 13 must be performed using formula [1]. But, the number of experiments should be multiples of 2 and 3 which indicate that minimum 18 experiments are required. Minitab 17 statistical software also suggested similar OA when data regarding their parameters and levels was given as input. On the other hand, the full factorial of design the experiments would have increased to 486 which would result in wastage of time, material and cost.

In present study, the percentage deviation in dimensions has been considered as response so as to minimize the error during calculation of SN ratios. It is calculated as:

$$\text{Percentage deviation} = \frac{\text{original (CAD) dimension} - \text{actual dimension}}{\text{original (CAD) dimension}} \times 100 \quad (2)$$

Table 3
Constant and variable parameters of FDM and VS apparatus.

Constant Parameters		
FDM Apparatus	Layer thickness (mm)	0.254
	Raster Angle	0°/90°
	Raster Width (mm)	0.4070
	Contour Width (mm)	0.4070
	Air Gap (mm)	0
	Extrusion Temperature (°C)	310°
Vapour Smoothing Apparatus	Cooling Temperature (°C)	0°
	Smoothing Temperature (°C)	48°

Variable Parameters					
		Symbol	Level		
			1	2	3
FDM Apparatus	Orientation Angle (°)	A	0°	90°	-
	Density	B	Normal	Sparse	Dense
Vapour Smoothing Apparatus	Precooling Time (min.)	C	10	15	20
	Smoothing Time (sec)	D	10	15	20
	Postcooling Time (min.)	E	10	15	20
	Number of Cycles	F	1	2	3

In case of uncontrolled noise factors, Signal to Noise ratio (SN ratio) is examined for selecting the robust experimental design. Signal to Noise ratio measures the sensitivity of response being investigated in controlled manner with respect to the external noise factors which are uncontrolled. Thus, signal to noise ratio has been calculated using smaller is better characteristic since aim is to reduce the dimensional variability (percentage deviation) in present context. The signal to noise ratio has been calculate using formula [3]:

$$\frac{S}{N} = -10\, Log_{10}\frac{1}{n}\left(\sum y^2\right) \quad (3)$$

where y is output response and n is number of observations.

The Tauchi's $_{L18}$ OA has been shown in Table 4 where columns represents input parameters while each row denotes a test condition which is created by combination of different levels of the input parameters. The orientation angle (A) with two levels has been assigned to first column; part density (B) being assigned to second column while interaction of parameter A and B was assigned to third column. The study of interactions between various input

Table 4
Taguchi's L_{18} orthogonal array.

Column No.	1	2	3	4	5	6	7	8	9	10	11
Exp. No.	A	B	AXB	C	D	AXD	BXD	CXD	E	DXE	F
1	1	1	1	1	1	1	1	1	1	1	1
2	1	1	1	2	2	2	2	3	2	3	2
3	1	1	1	3	3	3	3	2	3	2	3
4	1	2	2	1	1	1	2	1	2	2	2
5	1	2	2	2	2	2	3	3	3	1	3
6	1	2	2	3	3	3	1	2	1	3	1
7	1	3	3	1	2	2	1	2	1	2	3
8	1	3	3	2	3	3	2	1	2	1	1
9	1	3	3	3	1	1	3	3	3	3	2
10	2	1	2	1	3	3	3	3	3	2	2
11	2	1	2	2	1	2	1	2	1	1	3
12	2	1	2	3	2	1	2	1	2	3	1
13	2	2	1	1	2	1	3	2	3	1	1
14	2	2	1	2	3	3	1	1	1	3	2
15	2	2	1	3	1	2	2	3	2	2	3
16	2	3	3	1	3	3	2	3	2	1	3
17	2	3	3	2	1	2	3	2	3	3	1
18	2	3	3	3	2	1	1	1	1	2	2

parameters has been facilitated by line graph which greatly increases the accuracy of assigning proper columns. The line graph consists of circles, numbers and lines; where circle and number represents a factor (Fig. 4). The line connecting two dots indicates interaction. The number assigned to connecting line represents column number where interaction effect will be compounded [20]. The experiments were carried out in random order to minimize the effect of variation in temperature of vapours, heaters and cooling coils with time. Moreover three replications of each experiment were performed to minimize the random error in measurements. Thus, arithmetic average of three readings was considered as mean value.

3. Results and discussions

3.1. Data analysis

The mean values of Head Diameter before and after vapour smoothing have been shown in Table 5. The percentage deviation for both the cases has been calculated alongwith standard error and standard deviation to evaluate the uncertainty in measurements.

The standard deviation (SD) is best tool to estimate the distribution of data around mean value and not affected by extreme values. It can be calculated as:

$$SD = \sqrt{\frac{1}{N}\sum_{i=1}^{N}(X_i - \mu)^2} \tag{4}$$

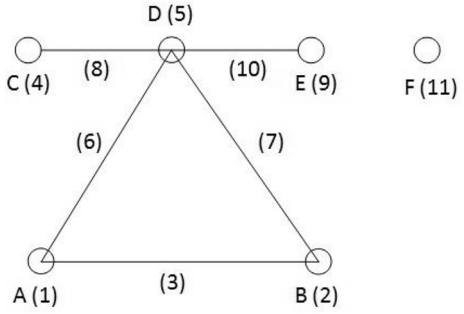

Fig. 4. Line graph for L_{18} orthogonal array.

The standard error (SE) measures deviation of calculated mean from actual mean values. The smaller the standard error proves that calculated mean strongly represents the actual value. It can be calculated as:

$$SE = \frac{SD}{\sqrt{N}} \tag{5}$$

where N is number of observations, μ is mean and x is measured value. The experiments are replicated for three times which gives N = 3 for present calculations.

The negative deviation in head diameter of FDM parts has been observed after fabrication (before vapour smoothing) which indicated under sizing. The FDM extrusion nozzle deposits the plastic in semi-molten condition which undergoes immediate shrinkage after cooling. Similar shrinkage phenomenon has been experienced by previous researchers [21–23]. Moreover, the effect of shrinkage is higher in case of replicas fabricated at 0° orientation angle. The percentage deviation in dimensions has been found lower in case of replicas fabricated at 90° orientation angle. In general, the slight difference in dimensional accuracy has been experienced with variation orientation angle [7,9]. The data showed further shrinkage in head diameter after vapour smoothing which further increases the percentage deviation. It can be noted from Table 5 that the standard deviation and standard error in measurements after vapour smoothing are reduced. This indicates higher accuracy in measurements after vapour smoothing of replicas.

On the hand, data related to Neck thickness indicates positive deviation i.e. actual neck thickness is higher than CAD dimensions (Table 6). The neck profile has intricate design features with rectangular cross-section and curved edges. Also, the thickness of neck continuously varies along the axis which generated approximation error in FDM extrusion nozzle. It can be noted that dimensions of replicas fabricated at 0° are built largely oversized as compared to 90° orientation angle. The reason lies behind manufacturing conditions at different orientation angles. The weld seam appears on neck section of replicas fabricated at 0° whereas weld seam is absent in 90° angle. Generally, both these angle are best for dimensional accuracy but little variation is found depending upon part geometry. The shrinkage in neck thickness after vapour smoothing process proved beneficial. In this case, the percentage deviation is reduced in all the 18 replicas when compared to deviation before vapour smoothing. Also, the standard deviation and standard error are reduced accordingly.

The stem thickness has been measured on stem length of replica at location 3. The thickness of stem section is measured before and after smoothing and compared individually with CAD dimension in Table 7. The sloping profile of stem section along the length with varying width and thickness at each point led to approximation error with oversized dimensions. Moreover, there is higher impact of stair case effect in case of 0° orientation angle. In 0° orientation angle conditions, the extrusion nozzle deposits material on small patch of cross-section as replica is aligned horizontal on the base. After wards, nozzle has to be raised to fabricate next cross-section with higher thickness which led to stair-stepping or staircase effect. On the other hand, parts are aligned vertically in 90° orientation angle which eliminated the risk of staircase effect. However, this phenomenon is not generalized and entirely case specific which differs depending upon part geometry.

After smoothing, the dimensions are reduced as vapour smoothing causes slight shrinkage on part dimensions irrespective of part geometry as deduced from Tables 5–7. It can be noted that after vapour smoothing, the standard deviation and standard error in observations were reduced during measurements of all the three features. Thus, the vapour smoothing process increases the

Table 5
Initial and final measurements of head diameter.

Head Diameter (CAD data = 12.0524 mm)										
Exp.	Before smoothing				After smoothing					
	Mean	SD	SE	% deviation	Mean	SD	SE	% deviation	SN ratio	IT Grade
1	12.0126	0.0032	0.0018	0.33	11.9981	0.0020	0.0011	0.45	6.9357	IT10
2	12.0128	0.0035	0.0020	0.33	11.9608	0.0019	0.0010	0.76	2.3837	IT11
3	12.0125	0.0033	0.0019	0.33	11.8981	0.0018	0.0010	1.28	−2.1442	IT12
4	12.0122	0.0033	0.0019	0.33	11.9776	0.0021	0.0012	0.62	4.1522	IT11
5	12.0125	0.0032	0.0018	0.33	11.8957	0.0017	0.0009	1.30	−2.2789	IT12
6	12.0127	0.0036	0.0021	0.33	11.8667	0.0017	0.0009	1.54	−3.7504	IT13
7	12.0127	0.0033	0.0019	0.33	11.9499	0.0018	0.0010	0.85	1.4116	IT11
8	12.0128	0.0035	0.0020	0.33	11.8848	0.0017	0.0009	1.39	−2.8603	IT12
9	12.0126	0.0033	0.0019	0.33	12.0066	0.0019	0.0010	0.38	8.4043	IT10
10	12.0331	0.0023	0.0013	0.16	11.9391	0.0009	0.0005	0.94	0.5374	IT11
11	12.0333	0.0026	0.0015	0.16	12.0270	0.0010	0.0005	0.21	13.5556	IT8
12	12.0331	0.0024	0.0014	0.16	12.0222	0.0011	0.0006	0.25	12.0412	IT9
13	12.0328	0.0025	0.0014	0.16	12.0186	0.0011	0.0006	0.28	11.0568	IT9
14	12.0326	0.0025	0.0014	0.16	11.9620	0.0009	0.0005	0.75	2.4988	IT11
15	12.0326	0.0023	0.0013	0.16	12.0066	0.0011	0.0006	0.38	8.4043	IT10
16	12.0328	0.0026	0.0015	0.16	11.9535	0.0009	0.0005	0.82	1.7237	IT11
17	12.0330	0.0024	0.0014	0.16	12.0210	0.0010	0.0005	0.26	11.7005	IT9
18	12.0325	0.0024	0.0014	0.16	12.0090	0.0010	0.0005	0.36	8.8739	IT9

Table 6
Initial and final measurements of Neck Thickness.

Neck Thickness (CAD data = 7.7458 mm)										
Exp.	Before smoothing				After smoothing					
	Mean	SD	SE	% deviation	Mean	SD	SE	% deviation	SN ratio	IT Grade
1	7.8674	0.0045	0.0026	1.57	7.8312	0.0029	0.0016	1.10	−0.8279	IT12
2	7.8650	0.0042	0.0024	1.54	7.7946	0.0026	0.0015	0.63	4.0132	IT10
3	7.8666	0.0046	0.0026	1.56	7.7622	0.0028	0.0016	0.21	13.5556	IT8
4	7.8643	0.0043	0.0024	1.53	7.8188	0.0031	0.0017	0.94	0.5374	IT11
5	7.8644	0.0044	0.0025	1.53	7.7862	0.0028	0.0016	0.52	5.6799	IT10
6	7.8681	0.0045	0.0026	1.58	7.7660	0.0029	0.0016	0.26	11.7005	IT9
7	7.8658	0.0045	0.0026	1.55	7.7861	0.0030	0.0017	0.52	5.6799	IT10
8	7.8666	0.0046	0.0026	1.56	7.7652	0.0029	0.0016	0.25	12.0412	IT8
9	7.8682	0.0042	0.0024	1.58	7.8140	0.0028	0.0016	0.88	1.1103	IT11
10	7.7656	0.0031	0.0017	0.25	7.7552	0.0017	0.0009	0.12	18.4164	IT7
11	7.7655	0.0032	0.0018	0.25	7.7606	0.0018	0.0010	0.19	14.4249	IT8
12	7.7654	0.0028	0.0016	0.25	7.7622	0.0015	0.0008	0.21	13.5556	IT8
13	7.7654	0.0030	0.0017	0.25	7.7576	0.0017	0.0009	0.15	16.4782	IT7
14	7.7656	0.0029	0.0016	0.25	7.7544	0.0019	0.0011	0.11	19.1721	IT7
15	7.7655	0.0030	0.0017	0.25	7.7599	0.0014	0.0008	0.18	14.8945	IT8
16	7.7655	0.0028	0.0016	0.25	7.7498	0.0019	0.0011	0.05	26.0206	IT5
17	7.7654	0.0028	0.0016	0.25	7.7630	0.0019	0.0011	0.22	13.1515	IT8
18	7.7655	0.0029	0.0016	0.25	7.7591	0.0015	0.0008	0.17	15.3910	IT8

Table 7
Initial and final measurements of Stem Thickness.

Stem thickness (CAD data = 6.6202 mm)										
Exp.	Before smoothing				After smoothing					
	Mean	SD	SE	% deviation	Mean	SD	SE	% deviation	SN ratio	IT Grade
1	6.8642	0.0127	0.0073	3.68	6.8413	0.0066	0.0038	3.34	−10.4749	IT14
2	6.8640	0.0131	0.0075	3.68	6.6970	0.0069	0.0039	1.16	−1.2892	IT12
3	6.8644	0.0127	0.0073	3.68	6.6329	0.0074	0.0042	0.19	14.4249	IT7
4	6.8644	0.0127	0.0073	3.68	6.7912	0.0070	0.0040	2.58	−8.2324	IT13
5	6.8642	0.0129	0.0074	3.68	6.6614	0.0065	0.0037	0.62	4.1522	IT10
6	6.8639	0.0133	0.0076	3.68	6.6832	0.0072	0.0041	0.95	0.4455	IT11
7	6.8642	0.0132	0.0076	3.68	6.6621	0.0068	0.0039	0.63	4.0132	IT10
8	6.8643	0.0130	0.0075	3.68	6.7276	0.0072	0.0041	1.62	−4.1903	IT12
9	6.8642	0.0128	0.0074	3.68	6.7911	0.0074	0.0042	2.58	−8.2324	IT13
10	6.7231	0.0040	0.0023	1.55	6.6235	0.0034	0.0019	0.05	26.0206	IT4
11	6.7233	0.0036	0.0020	1.55	6.6409	0.0032	0.0018	0.31	10.1728	IT9
12	6.7233	0.0036	0.0020	1.55	6.6335	0.0040	0.0023	0.24	12.3958	IT8
13	6.7232	0.0038	0.0021	1.55	6.6382	0.0036	0.0020	0.27	11.3727	IT8
14	6.7232	0.0040	0.0023	1.55	6.6315	0.0037	0.0021	0.17	15.3910	IT7
15	6.7232	0.0037	0.0021	1.55	6.6786	0.0036	0.0020	0.88	1.1103	IT11
16	6.7233	0.0039	0.0022	1.55	6.6223	0.0038	0.0022	0.03	30.4576	IT4
17	6.7234	0.0039	0.0022	1.55	6.6945	0.0033	0.0019	1.12	−0.9844	IT11
18	6.7233	0.0040	0.0023	1.55	6.6713	0.0032	0.0018	0.77	2.2702	IT11

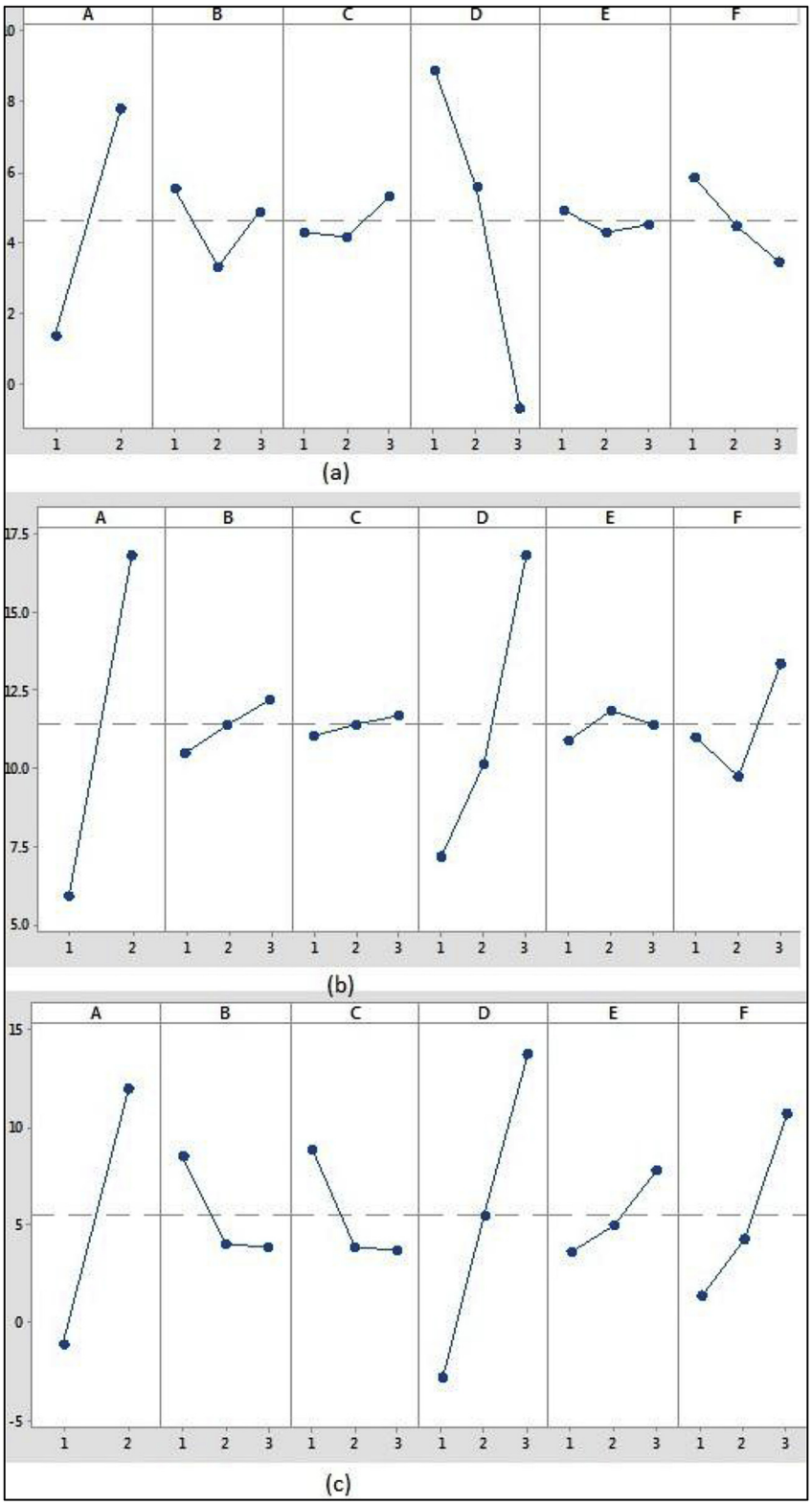

Fig. 5. Main effects plot of SN ratios for (a) head diameter (b) neck thickness (c) stem thickness.

measurement accuracy besides enhancing surface finish of replicas.

The international tolerance (IT) grades are used by industries to classify the process capability and precision of manufacturing process in terms of dimensional accuracy. Using designated IT grade formula, the grade is assigned to part features depending upon given tolerance and size. The IT grades are calculated to quantify the efficacy of vapour smoothing process for commercial use. The IT grades of head diameter, neck thickness and stem thickness are calculated for each experiment. The measurement data has been used to calculate the tolerance unit n that further derives standard

tolerance factor i as defined in ISO standard UNI EN 20286-1 [24]. The standard tolerances corresponding to IT grades (IT-5 to IT-18) for the linear dimensions (upto 500 mm) have been evaluated considering standard tolerance factor i (μm) given by the formula:

$$i = \left(0.45 \times D^{1/3}\right) + (0.001 \times D) \quad (6)$$

where D is the geometric mean of dimension in mm.

The standard tolerance factor depends upon mean diameter of thickness of given part feature and not separately evaluated for each nominal size, but it is common for the whole range of nominal sizes. Afterwards, the standard tolerance unit n for the nominal thickness is evaluated as:

$$n = 1000(D_{JN} - D_{JM})/i \quad (7)$$

where D_{JN} is original (CAD) dimension and D_{JM} is actual dimension.

Thus, the IT grade for individual experiment can be acquired from IT grade chart corresponding to standard tolerance unit. During measurements of three features of hip replicas, the IT grades are tabulated in last column of Tables 5–7 which varies from IT grade 4 to 13. The larger value of IT grade indicates larger tolerance as per industrial standards.

3.2. Effect of process parameters on dimensional accuracy

The SN ratios for percentage deviation after vapour smoothing of hip replicas are calculated for three dimensional features shown in Tables 5–7. The main effects plots of SN ratios (Fig. 5) for the investigated parameters are drawn for three dimensional features individually. Generally, the major of influence of orientation angle and smoothing time has been noted for all the three cases.

It is evident from Fig. 5 that parameter A and D make noticeable changes in mean SN ratios whereas change is insignificant for parameters B, C, E and F. As the orientation angle changes from 0° to 90°, the SN ratio increases from level 1 to 2. This indicates that vertical positioning of hip implant replicas during fabrication yields minimum dimensional variation. Although, dimensional accuracy for 90° orientation angle was higher even before smoothing, but it is more refined after vapour smoothing process. On the other hand, smoothing time (D) affects the SN ratios differently.

The SN ratios for head diameter measurements (Fig. 5a) decrease with increase in smoothing time as the larger smoothing time imparts further shrinkage in diameter. But, the SN ratio of neck thickness (Fig. 5b) and stem thickness (Fig. 5c) increases with smoothing time because these dimensions are already over-sized. Thus, the increase in smoothing time improves dimensional accuracy of neck and stem sections.

ANOVA statistical tool has been adopted by numerous researchers for analysis as it eliminates the limitations of graphical assessment. The F-values for each parameter have been compared with F-table values at 95% confidence level ($F_{0.05\ (2,12)} = 3.89$) as shown in Table 8. The degrees of freedom of parameters and error terms represent column number and row number respectively which help to locate values from F-table. The parameters having F-value higher than F-table value are considered as significant [20]. Alternatively, the parameters having p-values less than 0.05 (at 95% confidence level) are significant. In ANOVA analysis, both F-values and P-values yield similar conclusions.

The similar conclusions are endorsed by ANOVA tests performed on mean SN ratios of three dimensional features (Tables 8–10). In all the ANOVA tables, the F-values of parameters A and D are more than F-table values, which indicated that orientation angle and smoothing time have maximum influence on response. For neck section (Table 9), the orientation angle has maximum contribution of 59.78% whereas head and stem dimensions are highly influenced by smoothing time with contribution of 51.74% and 37.28%

Table 8
ANOVA results for SN ratios of percentage deviation in head diameter.

Source	DoF	Seq SS	Seq MS	F-Value	P-Value	Percentage Contribution	Significance
A	1	187.783	187.783	22.23	0.042	34.58	Yes
B*	2	15.306	7.653	0.91	0.525	2.8	No
C*	2	4.636	2.318	0.27	0.785	0.85	No
D	2	280.975	140.487	16.63	0.057	51.74	Yes
E*	2	1.147	0.574	0.07	0.936	0.21	No
F	2	17.525	8.763	1.04	0.491	3.2	Yes
A*B*	2	6.057	3.029	0.36	0.736	1.11	No
A*D*	2	12.683	6.341	0.75	0.571	2.33	No
Error	2	16.896	8.448			3.11	
Pooled Error	12	56.725				10.44	
Total	17	543.009				100	

*Pooled into error $F_{0.05\ (2,12)} = 3.89$.

Table 9
ANOVA results for SN ratios of percentage deviation in neck thickness.

Source	DoF	Seq SS	Seq MS	F-Value	P-Value	Percentage Contribution	Significance
A	1	533.715	533.715	145.55	0.007	59.78	Yes
B*	2	8.771	4.386	1.20	0.455	0.98	No
C*	2	1.275	0.638	0.17	0.852	0.14	No
D	2	290.819	145.409	39.66	0.025	32.57	Yes
E*	2	2.542	1.271	0.35	0.743	0.28	No
F	2	40.180	20.090	5.48	0.154	4.5	Yes
A*B*	2	3.077	1.538	0.42	0.704	0.34	No
A*D*	2	5.020	2.510	0.68	0.594	0.56	No
Error	2	7.334	3.667			0.82	
Pooled Error	12	28.019				3.13	
Total	17	892.732				100	

*Pooled into error $F_{0.05\ (2,12)} = 3.89$.

Table 10
ANOVA results for SN ratios of percentage deviation in stem thickness.

Source	DoF	Seq SS	Seq MS	F-Value	P-Value	Percentage Contribution	Significance
A	1	768.19	768.189	29.38	0.032	34.93	Yes
B*	2	83.87	41.936	1.60	0.384	3.81	No
C*	2	102.23	51.113	1.95	0.338	4.65	No
D	2	819.89	409.947	15.68	0.060	37.28	Yes
E*	2	53.62	26.812	1.03	0.494	2.43	No
F	2	271.46	135.728	5.19	0.162	12.34	Yes
A*B*	2	17.56	8.778	0.34	0.749	0.79	No
A*D*	2	29.90	14.950	0.57	0.636	1.35	No
Error	2	52.29	26.146			2.37	
Pooled Error	12	339.47				15.43	
Total	17	2199.01				100	

*Pooled into error $F_{0.05\ (2,12)} = 3.89$.

respectively. The other parameters are having negligible contribution and thus pooled in error. ANOVA tables indicated negligible effects of interactions between parameters A, B and D (Max. 2.33% contribution) on SN ratios and thus pooled into error. Other interaction effects are not included by Minitab statistical software due to their insignificance.

3.3. Smoothing phenomenon

The smoothing fluid vaporizes readily when heated and immediately reacts with upper surface of parts. The vapour does not enter deep inside the surface which is confirmed by non-significance of part density (parameter B) in ANOVA analysis. The chemical vapours lowers the glass transition temperature of ABS plastic which cause temporary and localised melting of upper layers. The layers re-settle as smooth surface under surface tension forces which tend to cover minimum surface area. The plastic material flows from peaks to deposit into valleys which ended as a smooth surface.

The downward movement (shrinkage) of upper plastic layers (at micro level) tend to reduce the overall dimensions of replicas as reported by previous researchers [12–15]. The smoothing phenomenon is sketched in Fig. 6 which also shows deviation between original and actual surfaces. Fig. 6a shows deviation in neck and stem thickness (linear) having over-sized dimension. After vapour smoothing, the layers reflow and settle as smooth surface which reduces the deviation (Fig. 6b). The replicas must be immediately cooled after smoothing to avoid over-heating which signifies the importance of post-cooling. On the other hand, the radial dimension (head diameter) is produced under-sized (Fig. 6c). After smoothing, the surface roughness is reduced but deviation increases in head diameter (Fig. 6d). The layer settlement and reduction in surface roughness improves the measuring accuracy of CMM which is confirmed by comparatively lower standard deviation and standard error values after smoothing. The probe of CMM accurately traces data points of smooth surface with minimum error.

The surface roughness profiles and SEM images have been acquired to validate the smoothing phenomenon and dimensional changes occurring during finishing process. The surface roughness profiles of replicas with orientation angle 90° before vapour smoothing process shows semi-circular profile on micro scale (Fig. 7c). The profiles showed considerable decrease in peak height after vapour smoothing (Fig. 7d). On the other hand 0° orientation

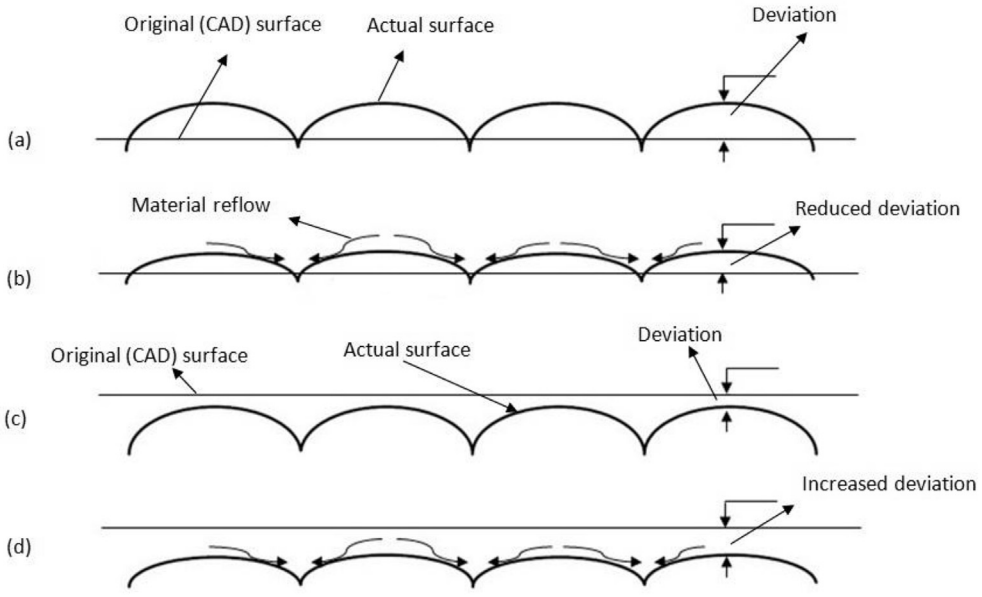

Fig. 6. Smoothing phenomenon and deviations in (a) stem thickness before smoothing (b) stem thickness after smoothing (c) head diameter before smoothing (d) head diameter after smoothing.

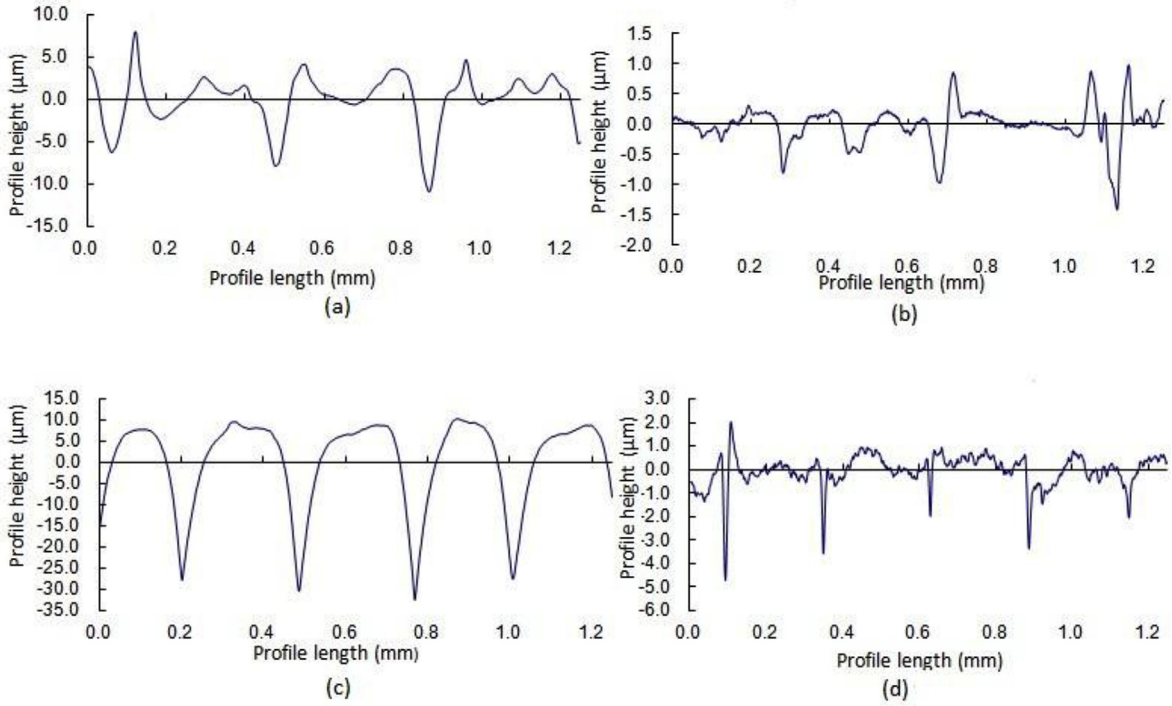

Fig. 7. Surface roughness profiles of replicas at orientation angle (a) 0° before smoothing (b) 0° after smoothing (c) 90° before smoothing (d) 90° after smoothing.

replicas have higher level of waviness before smoothing which is further disturbed after smoothing (Fig. 7a and b). However, the average surface roughness and peak height is reduced in both cases. But the replicas fabricated at 90° orientation angle have higher surface clarity which supports both Taguchi and ANOVA results. The similar semi-circular profile is clearly visible in SEM micrographs (Fig. 8a) before vapour smoothing but a plane surface is viewed after vapour smoothing (Fig. 8b). The shrinkage (smoothing phenomenon) tends to reduce both surface roughness and dimensions of linear and radial sections.

3.4. Optimization and confirmatory experiments

The minimum deviations are required for all the dimensional features of FDM replicas for mass production and consistency in final castings. It has been observed that the most significant parameters and percentage contribution for the three responses are different. Similarly, the optimum parameter level setting is different for three dimensional features. There are number of conflicting parameters that may influence the individual dimensional accuracy of part features. Thus, instead of optimizing

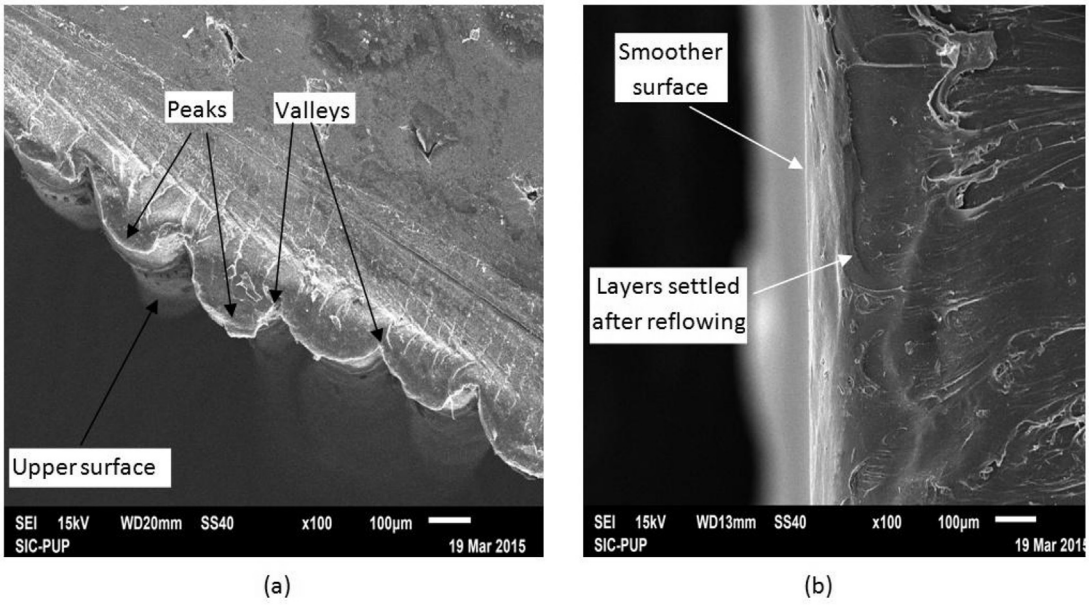

Fig. 8. SEM micrograph images (in transverse view) of ABS replicas (a) before smoothing (b) after smoothing.

Table 11
Constraints to parameters and optimum levels suggested by statistical software.

Parameter	Goal	Lower Limit	Upper Limit	Weight	Importance
Orientation Angle	Constraint to region	0°	90°	1	1
Part Density	Constraint to region	normal	dense	1	1
Pre-cooling time	Constraint to region	10 min	20 min	1	1
Smoothing time	Constraint to region	10 s.	20 s.	1	1
Post-cooling time	Constraint to region	10 min	20 min	1	1
No. of cycles	Constraint to region	1	3	1	1
SN Ratio (Head Diameter)	Maximize	−3.7504	13.5556	1	1
SN Ratio (Neck Diameter)	Maximize	−0.8279	26.0206	1	1
SN Ratio (Stem Thickness)	Maximize	−10.4749	30.4576	1	1

Optimum Values

Orientation Angle	Part Density	Pre-cooling time	Smoothing time	Post-cooling time	No. of cycles	SN Ratio (Head Diameter)	SN Ratio (Neck Diameter)	SN Ratio (Stem Thickness)	Desirability
90°	Solid-normal	10 min	15 s.	20 min	3	8.29134	16.3721	25.9731	0.734912

Table 12
Percentage deviations and IT grades of part features at optimum parameter setting.

Exp.	Head Diameter (CAD data) = 12.0524 mm			Neck Diameter (CAD data) = 7.7458 mm			Stem Thickness (CAD data) = 6.6202 mm		
	Head Diameter	% deviation	IT Grade	Head Diameter	Percentage deviation	IT Grade	Head Diameter	% deviation	IT Grade
1	12.0102	0.35	IT9	7.7621	0.21	IT8	6.6498	0.44	IT9
2	12.0099	0.35	IT9	7.7626	0.21	IT8	6.6474	0.41	IT9
3	12.0089	0.36	IT9	7.7622	0.21	IT8	6.6488	0.43	IT9
4	12.0095	0.35	IT9	7.7610	0.19	IT8	6.6492	0.43	IT9
5	12.0124	0.33	IT9	7.7593	0.17	IT8	6.6482	0.42	IT9
6	12.0115	0.34	IT9	7.7595	0.17	IT8	6.6475	0.41	IT9
7	12.0088	0.36	IT9	7.7615	0.20	IT8	6.6487	0.43	IT9
8	12.0094	0.35	IT9	7.7598	0.18	IT8	6.6472	0.40	IT9

individual response in an arbitrary manner, it is required to obtain the single parameter setting that simultaneously minimizes the deviations in all the dimensional features. The response optimization module of Minitab software has been utilized to achieve optimized set of process parameters. The constraints, weight and importance is entered for each process parameter along with upper and lower limits. The objective is to achieve maximum SN ratios for each response and thus best levels of each parameter are suggested along with desirability (Table 11).

The confirmation tests are performed to validate the predictions and evaluate the repeatability of FDM-VS processes. The eight replicas are again fabricated at optimum parameter settings and the dimensions of three features are measured after vapour smoothing process. The percentage deviation between actual and original dimensions (CAD data) is calculated alongwith corresponding IT grade as shown in Table 12. The maximum percentage deviation of 0.44% has been observed in stem thickness while minimum 0.17% in neck thickness. The IT grades are improved and found consistent for each feature which indicates sound repeatability and reproducibility of FDM-VS processes.

4. Conclusions

- This research work presents a systematic methodology for creating a robust experimental design for FDM-VS process for improving the dimensional accuracy of various features of hip implant replicas.
- The three intricate part features are studied; dimensions are measured before and after vapour smoothing process and compared with original CAD dimensions.
- The initial measurements of head diameter reported undersizing radial dimensions whereas linear dimensions (stem and neck thickness) are made oversized.
- The vapour smoothing process caused further shrinkage in both linear and radial dimensions as upper plastic layers reflowed to settle as smooth surface. The increased smoothing time reduced deviations in neck and stem thickness while head diameter deviation is increased.
- The optimized level settings of parameters for best minimum deviation are acquired and confirmed through experiments.
- The results encourage for in-vivo and in-vitro testing of castings prepared through proposed route. Following these results, the methodology aiming to install customized biomedical implants in patients could be developed through FD-VS-IC processes.

The extension of the proposed methodology for the rapid manufacturing of innovative materials and structures [25–41] awaits attention.

References

[1] Standard, A.S.T.M. F2792–12a Stand Termin Addit Manuf Technol 2012;10.
[2] Bassoli E, Gatto A, Iuliano L, Grazia Violante M. 3D printing technique applied to rapid casting. Rapid Prototyp J 2007;13(3):148–55.
[3] Wang S, Miranda AG, Shih C. A study of investment casting with plastic patterns. Mater Manuf Process 2010;25(12):1482–8.
[4] Pattnaik S, Jha PK, Karunakar DB. A review of rapid prototyping integrated investment casting processes. Proceedings of the institution of mechanical engineers. Part L J Mater Des Appl 2014;228(4):249–77.
[5] Perez CL. Analysis of the surface roughness and dimensional accuracy capability of fused deposition modelling processes. Int J Prod Res 2002;40(12):2865–81.
[6] Noriega A, Blanco D, Alvarez BJ, Garcia A. Dimensional accuracy improvement of FDM square cross-section parts using artificial neural networks and an optimization algorithm. Int J Adv Manuf Technol 2013;69(9–12):2301–13.
[7] Weeren RV, Agarwala M, Jamalabad VR, Bandyophadyay A, Vaidyanathan R, Langrana N, et al. Quality of parts processed by fused deposition. In: Proceedings of the Solid Freeform Fabrication Symposium6; 1995, August. p. 314–21.
[8] Mohamed OA, Masood SH, Bhowmik JL. Optimization of fused deposition modeling process parameters: a review of current research and future

prospects. Adv Manuf 2015;3(1):42–53.
[9] Fodran E, Koch M, Menon U. Mechanical and dimensional characteristics of fused deposition modeling build styles. Solid Free Fabr Proc 1996, August: 419–42.
[10] Sorrentino R, Gherlone EF, Calesini G, Zarone F. Effect of implant angulation, connection length, and impression material on the dimensional accuracy of implant impressions: an in vitro comparative study. Clin implant Dent Relat Res 2010;12(1):63–76.
[11] Chohan JS, Singh R. Pre and post processing techniques to improve surface characteristics of FDM parts: a state of art review and future applications. Rapid Prototyp J 2017;23(3). In press.
[12] Galantucci LM, Lavecchia F, Percoco G. Experimental study aiming to enhance the surface finish of fused deposition modeled parts. CIRP Annals-Manufacturing Technol 2009;58(1):189–92.
[13] Kuo CC, Mao RC. Development of a precision surface polishing system for parts fabricated by fused deposition modeling. Mater Manuf Process 2016;31(8):1113–8.
[14] Garg A, Bhattacharya A, Batish A. On surface finish and dimensional accuracy of FDM parts after cold vapour treatment. Mater Manuf Process 2016;31(4): 522–9.
[15] Espalin D, Medina F, Arcaute K, Zinniel B, Hoppe T, Wicker R. Effects of vapour smoothing on ABS part dimensions. In: Proceedings from rapid 2009 conference & exposition; 2009, May [Schaumburg, IL].
[16] ISO, P., 10360–2 Geometrical Product Specifications (GPS). Acceptance tests and periodic coordinate measuring machines (CMM). Part 2.
[17] Standard ISO. Geometrical Product Specifications (GPS)–Surface texture: profile method–Terms, definitions and surface texture parameters. Int Organ Stand 1997;4287.
[18] Stratasys Inc. Finishing touch smoothing station- service manual. 2010.
[19] Microcare-Safety Data Sheet 2009, http://www.stratasys.com/~/media/Main/Secure/MSDS/Smoothing_Station_Fluid/MSDS_Smoothing_Station_Fluid.pdf (Accessed 10 May 2015).
[20] Krishnaiah K, Shahabudeen P. Applied design of experiments and Taguchi methods. PHI Learning Pvt. Ltd; 2012.
[21] Wang TM, Xi JT, Jin Y. A model research for prototype warp deformation in the FDM process. Int J Adv Manuf Technol 2007;33(11–12):1087–96.
[22] Singh J, Singh R, Singh H. Repeatability of linear and radial dimension of ABS replicas fabricated by fused deposition modelling and chemical vapour smoothing process: a case study. Measurement 2016;94:5–11.
[23] Gurrala PK, Regalla SP. Multi-objective optimisation of strength and volumetric shrinkage of FDM parts: a multi-objective optimization scheme is used to optimize the strength and volumetric shrinkage of FDM parts considering different process parameters. Virtual Phys Prototyp 2014;9(2):127–38.
[24] UNI, E. ISO System of limits and fits. 20286–20291 Bases Toler deviations fits 1995.
[25] Singh R, Singh S, Fraternali F. Development of in-house composite wire based feed stock filaments of fused deposition modelling for wear-resistant materials and structures. Compos Part B, Eng 2016;98:244–9.
[26] Singh R, Kumar R, Feo L, Fraternali F. Friction welding of dissimilar plastic/polymer materials with metal powder reinforcement. Compos Part B, Eng 2016;101:77–86.
[27] Ascione L, Fraternali F. A penalty model for the analysis of composite curved beams. Comput Struct 1992;45:985–99.
[28] Fraternali F, Reddy JN. A penalty model for the analysis of laminated composite shells. Int J Solids Struct 1993;30:3337–55.
[29] Fraternali F. Free discontinuity finite element models in two-dimensions for in-plane crack problems. Theor Appl Fract Mech 2007;47:274–82.
[30] Farina I, Fabbrocino F, Carpentieri G, Modano M, Amendola A, Goodall R, et al. On the reinforcement of cement mortars through 3D printed polymeric and metallic fibers. Compos Part B, Eng 2016;90:76–85.
[31] Farina I, Fabbrocino F, Colangelo F, Feo L, Fraternali F. Surface roughness effects on the reinforcement of cement mortars through 3D printed metallic fibers. Compos Part B, Eng 2016;99:305–11.
[32] Schmidt B, Fraternali F. Universal formulae for the limiting elastic energy of membrane networks. J Mech Phys Solids 2012;60:172–80.
[33] Kim B, Doh JH, Yi CK, Lee JY. Effects of structural fibers on bonding mechanism changes in interface between GFRP bar and concrete Composites. Part B Eng 2013;45(1):768–79.
[34] Donnini J, Corinaldesi V, Nanni A. Mechanical properties of FRCM using carbon fabrics with different coating treatments. Compos Part B, Eng 2016;88:220–8.
[35] Jia Y, Chen Z, Yan W. A numerical study on carbon nanotube pullout to understand its bridging effect in carbon nanotube reinforced composites. Compos Part B, Eng 2015;81:64–71.
[36] Amendola A, Nava EH, Goodall R, Todd I, Skelton RE, Fraternali F. On the additive manufacturing and testing of tensegrity structures. Compos Struct 2015;131:66–71.
[37] Amendola A, Smith CJ, Goodall R, Auricchio F, Feo L, Benzoni G, et al. Experimental response of additively manufactured metallic pentamode materials confined between stiffening plates. Compos Struct 2016;142:254–62.
[38] Amendola A, Fabbrocino F, Feo L, Fraternali F. Dependence of the mechanical properties of pentamode materials on the lattice microstructure. ECCOMAS Congr 2016-Proc 7th Eur Congr Comput Methods Appl Sci Eng 2016;1: 2134–50.
[39] Amendola A, Carpentieri G, Feo L, Fraternali F. Bending dominated response of layered mechanical metamaterials alternating pentamode lattices and confinement plates. Compos Struct 2016;157:71–7.
[40] Fabbrocino F, Amendola A, Benzoni G, Fraternali F. Seismic application of pentamode lattices. Ingegneria Sismica/International J Earthq Eng 2016;1–2. ISSN: 0393-1420:62–71.
[41] Amendola A, Carpentieri G, de Oliveira M, Skelton RE, Fraternali F. Experimental investigation of the softening-stiffening response of tensegrity prisms under compressive loading. Compos Struct 2014;117:234–43.